

# FATIGUE OF NOTCHED STANDARD SPECIMENS – THE INFLUENCE OF THE STRESS GRADIENT ON THE S-N CURVE IN AL2024

S Sieberer<sup>1</sup>, J Homan<sup>2</sup> & M Schagerl<sup>1</sup>

<sup>1</sup>Institute of Structural Lightweight Design, Johannes Kepler University Linz, Altenberger Strasse 69, 4040 Linz, Austria

<sup>2</sup>Fatec Engineering, Prinses Christinastraat 6, 3958 VZ Amerongen, The Netherlands

## Abstract

The fatigue life of three designs of notched aluminium specimens with nominally similar stress concentration factor  $K_t$  is compared by experimental testing. A dependency of the fatigue life on the stress gradient is shown. By comparison to unnotched specimens, the fatigue stress concentration factor  $K_{t,f}$  can be obtained by applying a correction factor to the nominal  $K_t$ . Usual correction factors underestimate the effect by a large extent and should be re-evaluated to utilise the full potential of the material.

**Keywords:** Fatigue testing; Stress gradient; Notched specimens; Digital image correlation

## 1. Introduction

Aluminium-made parts remain integral to primary aircraft structures despite competition from fibre-reinforced composite materials. Well-understood material properties and good damage tolerance are amongst the benefits of using the aluminium alloy AL2024 in aircraft design. However, fatigue behaviour of the material is often calculated on the basis of unnotched specimen data, giving a material S-N curve, or on specific notched specimen data, where the geometry may have little in common with designed structural parts apart from the nominal stress concentration in static loading. Often such specimens feature one or more internal circular holes to yield a local stress raiser described by the stress concentration factor

$$K_t = \frac{\sigma_{\max}}{\sigma_{\text{nom}}} \quad (1)$$

where  $\sigma_{\max}$  is the maximum stress, and  $\sigma_{\text{nom}}$  is a nominal stress. It is widely known that the stress concentration of a hole in an infinite plate under plane-stress linear elastic conditions and for isotropic material is  $K_t=3$  [1]. For finite-width plates with a central hole, this stress concentrations reduces with the ratio of hole diameter  $d$  to width  $b$ . Analytical solutions for  $0 < d/b < 0.5$  were found by Howland [2] using series expansion and were more recently numerically evaluated by Filippini and co-workers [3]. Koiter [4] gave the lower limit of  $K_t$  as 2.0 for large circular holes in a strip by application of beam theory. To yield  $K_t < 2.0$ , elliptical holes with the major axis in the strip direction and largely different semiaxis lengths have to be used. These and other specimen geometries rely on a well-defined nominal stress, usually defined as the applied force over the net cross-section.

Figure 1 shows a sketch of a finite-width plate with a hole and the stress distribution under linear-elastic assumptions in the net section under uniform far-field stress in y-direction. For most engineering metals, material plasticity and strain hardening reduce the effect of stress concentrations under large static loads, and the failure load of the notched specimen can be approximated by the material strength of the net section. Under fatigue however, loading of the material is - with the exception of low cycle fatigue - mostly in the elastic range, and the linear elastic stress concentration has to be considered. Theories to adapt the stress concentration concept to fatigue load cases were derived e.g. by Neuber [5], Siebel and Stieler [6], and Peterson [7]. They all use semi-empirical models to match experimental data to the theory of stress concentrations. More generally, there may not be a

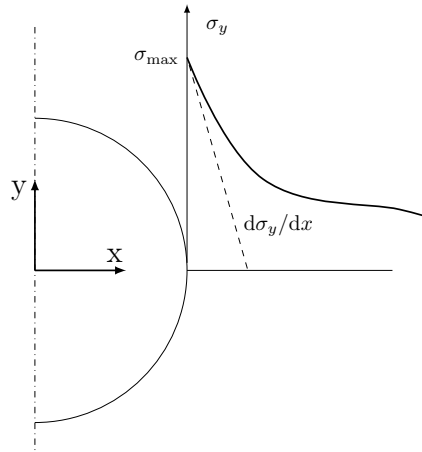


Figure 1 – Stress in the net section of a finite plate with hole under uniform tension and the stress gradient.

nominal stress to compare the notch stress to, and local stress maxima have to be fatigue-checked by other means. The method by Siebel and Stieler uses the so-called relative stress gradient,  $\chi$ , which is the maximum gradient of the stress concentration relative to the maximum stress at the notch and given by

$$\chi = \frac{d\sigma_y/dx}{\sigma_{\max}} \quad (2)$$

It states that physically, a larger gradient hinders micro-crack formation and growth to macro-cracks, and is known as the support-effect [8]. Other researchers, e.g. Schijve [9], explain the beneficial effect of a large stress gradient as a size-effect. Both explanations are – to the authors views – viable and a combination of both is probably causing the life-extending effect.

The industrial standard FKM [10] gives a refined method based on [6] using  $\chi$  to yield the fatigue stress concentration factor  $K_{t,f}$  as

$$K_{t,f} = n_\sigma K_t \quad (3)$$

where  $n_\sigma$  is called *support factor* and is semi-empirically obtained for different materials and yield strengths from  $\chi$ .

In this contribution, an experimental investigation into the effect of different relative stress gradients in specimens made of the same plate of AL2024 T351 material with similar size and nominal stress concentration is performed. The fatigue life is tested for samples under constant amplitude tensile-tensile fatigue loading. Results show that there is a general effect of life-increase with higher relative stress gradient, which may have to be considered even on the specimen level. The beneficial effect of  $\chi$  in the test samples is much larger than so far considered in application formulas, and for best use of material fatigue strength, tested parameters for given material should be used.

## 2. Specimens and Experimental Set-up

### 2.1 Specimen Designs and Loads

In the experimental series, three notched specimen designs were considered, (i) a HSB specimen [11], (ii) a NACA-type specimen [12], and (iii) a elliptical-hole specimen, see Figure 1. The HSB and NACA design have reported stress concentration factors  $K_t = 2.0$ , however, the finite element analysis (FEA) of the NACA specimen presented later in this paper showed a slightly higher  $K_t = 2.1$ . The elliptical-hole specimen was designed to a  $K_t = 2.0$  using static FEA. Table 1 gives the FEA obtained stress concentration factors and relative stress gradients. Additionally, an unnotched specimen design with  $K_t = 1.0$  was tested for reference S-N data. All test series were performed on the same test rig with similar environmental laboratory conditions. The material used in the tests was AL2024-T351 with a thickness of  $t=4.83\text{mm}$ . All specimens were manufactured to be loaded in the rolling direction. The holes were cut by waterjet-cutting. To reduce surface influence, all surfaces in the hole area were then sanded and finely polished.

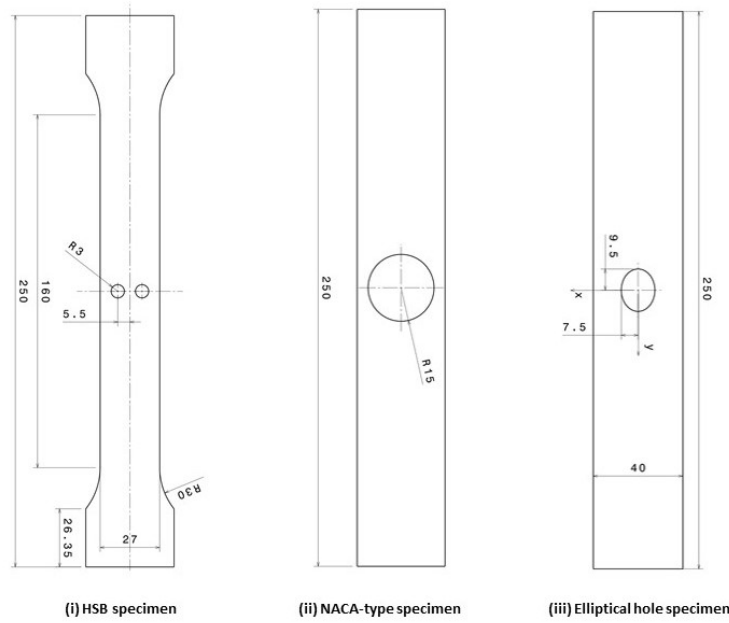


Figure 2 – Specimen designs used in experimental testing.

## 2.2 Test Set-up and Evaluation

Experimental testing was carried out on a Zwick-Roell hydraulic test rig with nominal rating of 100kN. The hydraulic cylinder is shown in Figure 3. Figure 4 shows the MTS 647 hydraulic grips used to clamp the specimens and a fractured specimen after testing. Quasi-static experiments were performed under displacement-control with unnotched specimens to obtain material stress-strain curves and values for the material yield and tensile strength. Fatigue testing was performed under load control with load ratio  $R=0.1$  and cyclic frequencies ranging from 5 Hz to 15 Hz, with lower test frequency at higher loads. The applied force was measured by the load cell of the test rig, and displacement by the internal sensor of the hydraulic cylinder. Load levels were chosen to yield estimated fatigue lives in the high-cycle fatigue range from  $N_f = 10^4$  to  $5 \times 10^5$  cycles. Resulting stress levels did not yield large local plastic deformation since the effect of these deformations is not part of the investigation. For an analysis of elasto-plastic fatigue of the elliptical specimens, see [13]. Longer fatigue lives were equally not in the focus of the investigation.

The evaluation of the fatigue tests was performed according to Basquin [14], plotting the stress amplitude over cycles to failure on a log-log scale. Equally, the regression line of each specimen design was obtained in the log-log space using

$$\log N_f = a - b \log \sigma_a \quad (4)$$

where  $N_f$  is the number of cycles to failure,  $\sigma_a$  is a stress amplitude, and  $a$  and  $b$  are the regression parameters. For better comparison between the unnotched and notched specimens, the local stress amplitudes at the stress concentration were used for the notched specimens. Statistical significance of the results was checked assuming log-normal distribution of results with constant standard deviation over the sample [15].

## 3. Results and Discussion

### 3.1 Finite Element Results

A FEA was performed in Abaqus CAE2017 to give the  $K_t$  and  $\chi$  values for the specimens. 2d-models with nominal specimen geometries and assuming plain stress conditions were set-up using 2nd order elements CPS8R and mesh refinement around the stress concentrations. The minimal mesh size at the hole is 0.05 mm for all models. A convergence study ensured the sufficient mesh fineness.

A nominal load resulting in  $\sigma_{nom}=10$  MPa was applied and linear elastic material with  $E=72000$  MPa and  $\nu=0.3$  used in the linear solution process. Post-processing showed the stress distribution around



Figure 3 – Test rig with hydraulic cylinder.

Specimen	$K_t$	$\chi$ in 1/mm
HSB design outside	2.02	0.80
HSB design inside	1.90	0.65
NACA design	2.11	0.32
Ellipse	2.00	0.23

Table 1 – Stress concentration and relative stress gradient for specimens from FEA.

the hole and the relative stress gradient perpendicular to the hole at the maximum stress location. These results are shown in Figure 5. Figures 6, 7, and 8 show the FEA obtained  $K_t$  and  $\chi$  values for the three notched specimen designs. The peak values at the hole are reported in Table 1.

Note that for the HSB design with two holes, there are four local stress maxima, symmetrically arranged about the central vertical plane. On the outside of the holes facing the specimen edge, there is the maximum stress and the  $K_t$  of 2.02. Facing the centre on the inside of the holes are secondary stress concentrations with lower  $K_t=1.90$ . Furthermore, the  $\chi$  values are also different,  $\chi=0.80$  on the outside and  $\chi=0.65$  on the inside.

### 3.2 Experimental Results

Static test data of the unnotched specimens are shown in Figure 9 for longitudinal (L) and transversal (T) material direction. The stress axis is normalised to the experimentally obtained material yield stress  $R_{el}$  in L-direction. In all presented test data, the local maximum stresses in the net section  $\sigma_{max}$  are normalised in this way to give the normalised load

$$L_{norm} = \frac{\sigma_{max}}{R_{el}} \quad (5)$$

For the fatigue testing, approximate load levels were defined for each specimen, and three specimens

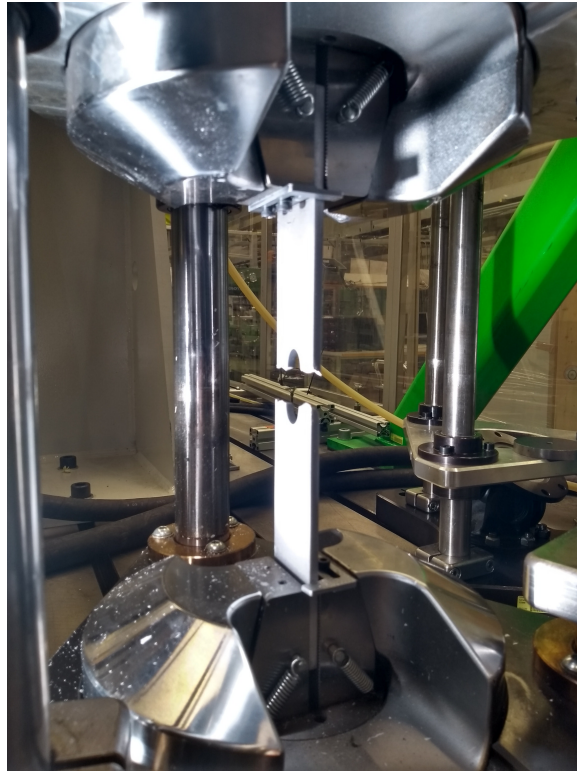


Figure 4 – Fractured specimen with elliptical hole in the test facility.

Load Levels	Unnotched	Ellipse	HSB	NACA
High	0.45	0.49	0.47	0.48
Medium	0.38	0.45	0.42	0.38
Low	0.30	0.30	0.30	0.30

Table 2 – Normalised stress amplitude levels used in fatigue testing.

were tested at each load level. Table 2 shows the normalised cyclic amplitudes, which were slightly different between specimen designs. Different stress levels are used to achieve the same local stress level at the notch per load level. Note that the testing data is restricted to the high cycle fatigue range.

Figures 10 and 11 show failed specimens for each design. Note the significant area of the fatigue crack perpendicular to the load direction present in each specimen. The remaining fracture area is taken up by the residual strength fracture, exhibiting a shear-type fracture at planes in 45° orientation to the load direction. The fatigue crack starts at one of the stress concentrations and usually, only one fatigue crack forms. However, in some HSB-design specimens, there are fatigue cracks on one outside section and in the central section. Reason for this may be that after the initial fatigue crack has formed, the residual cross-section for this specimen is large enough to allow the formation of a second fatigue crack before the remaining cross-section cannot support the cyclic load and the specimen fails.

The test data and S-N curves with normalised local stresses are shown in Figure 12. This means, the maximum stress at the stress concentration is used to give the stress amplitude value. For comparison, the unnotched specimen with  $K_t=1.0$  is included in the chart.

In material testing, often only one specimen design per stress concentration value is tested, see e.g. NACA or IASB reports, and the shortcomings of such an approach are visible in the separation of the three S-N curves of the notched specimens. There is not only one S-N curve for a notched design, but the different designs give different fatigue lives. It is therefore significant to know other parameters of the specimen, e.g. size or relative stress gradient. In Figure 12, the specimen with the largest  $\chi$  shows the longest life, i.e. there is a beneficial effect of the higher stress gradient. For the two

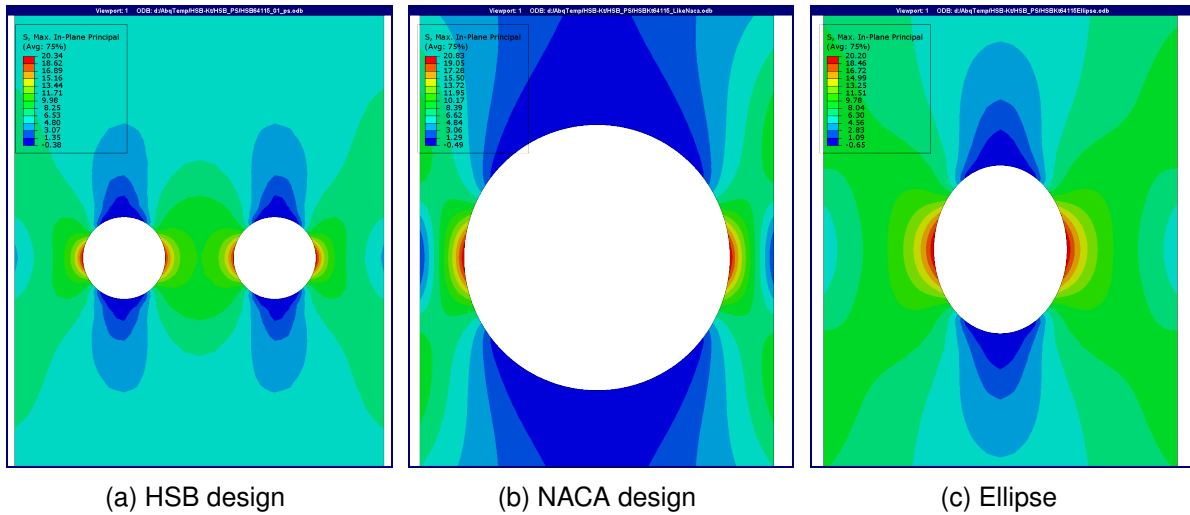


Figure 5 – FEA results of maximum principal stress fields in the specimens under nominal uniaxial stress  $\sigma_{nom}=10$  MPa.

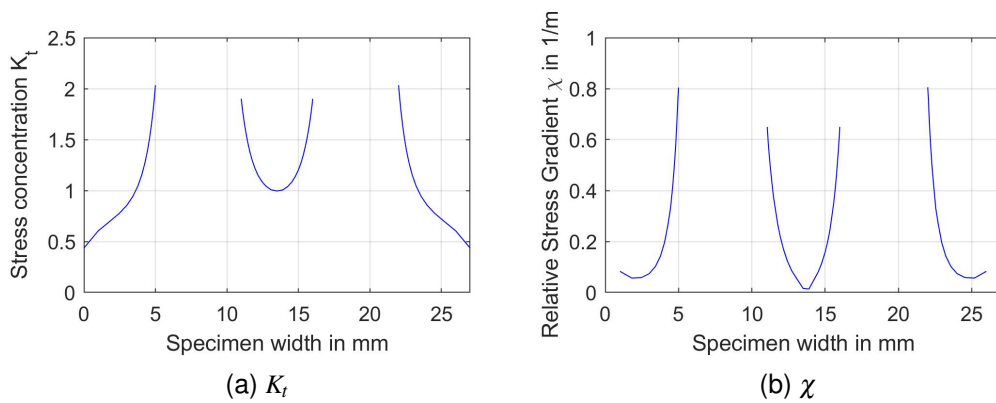


Figure 6 – FEA obtained graphs for  $K_t$  and  $\chi$  over the specimen width in the net section.

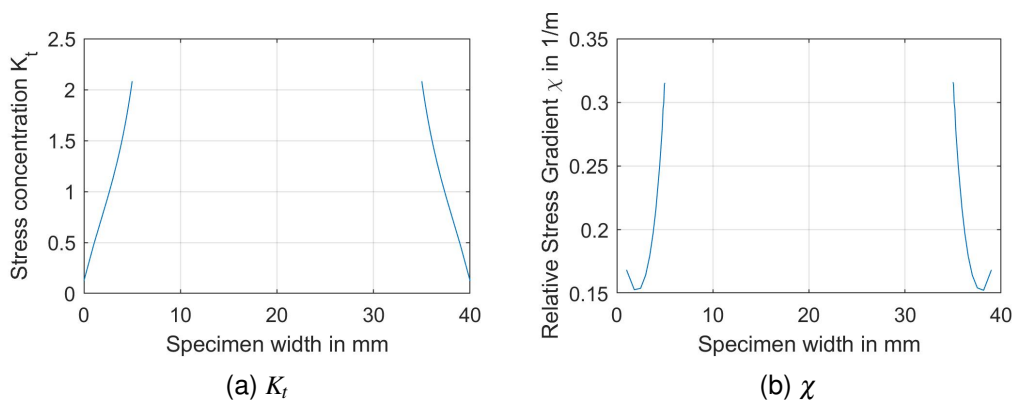


Figure 7 – FEA obtained graphs for  $K_t$  and  $\chi$  over the specimen width in the net section.

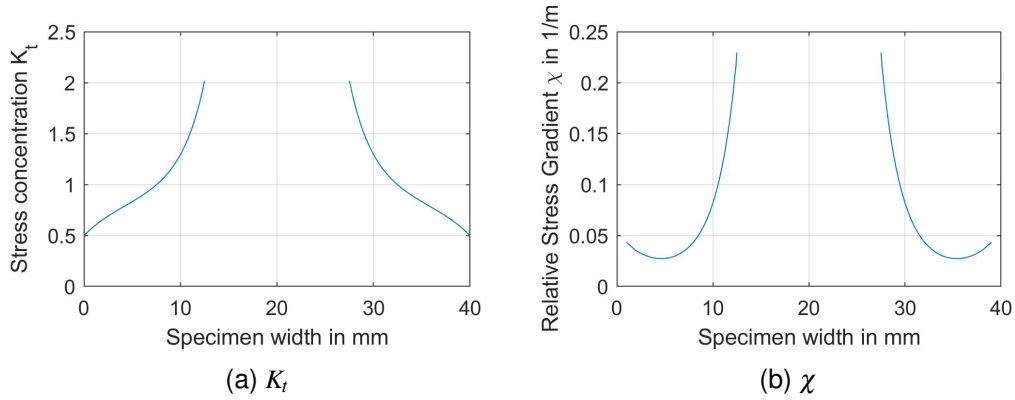


Figure 8 – FEA obtained graphs for  $K_t$  and  $\chi$  over the specimen width in the net section.

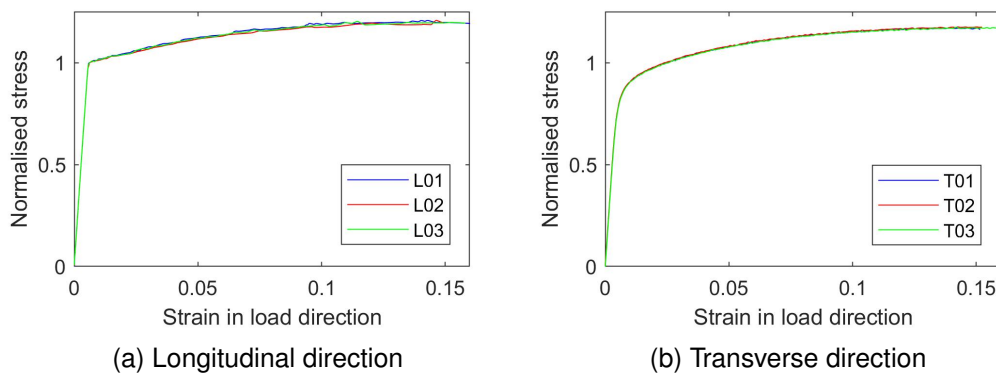


Figure 9 – Static stress-strain curves in longitudinal (L) and transversal (T) direction. The yield stress in L-direction was used to normalised the stress. The defined yield point from pre-tensioning is visible.

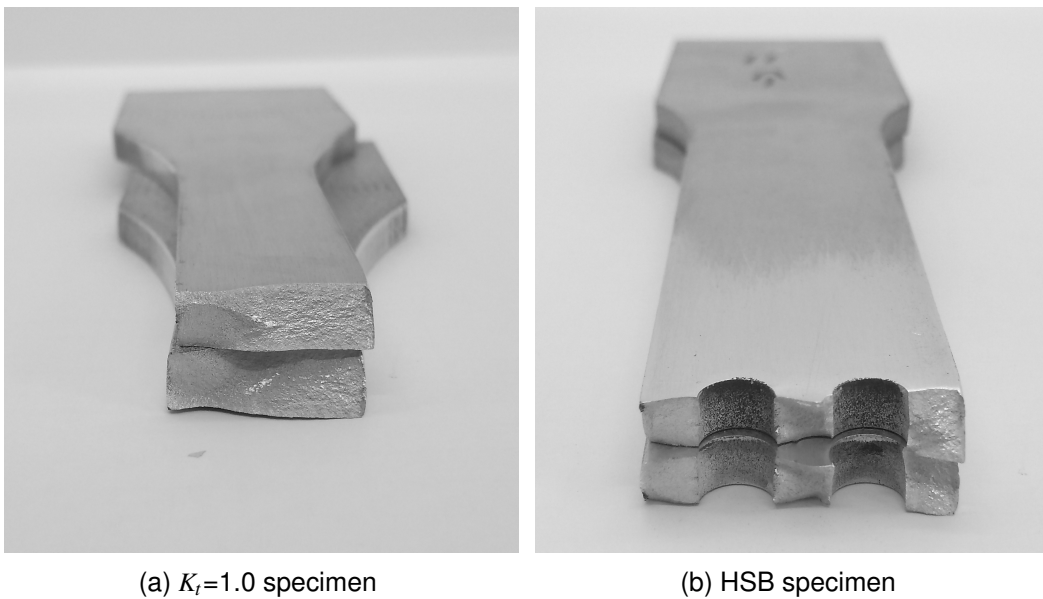


Figure 10 – Examples of failed specimens. There is an area of fatigue crack growth with the crack path perpendicular to the loading direction followed by a residual strength fracture.

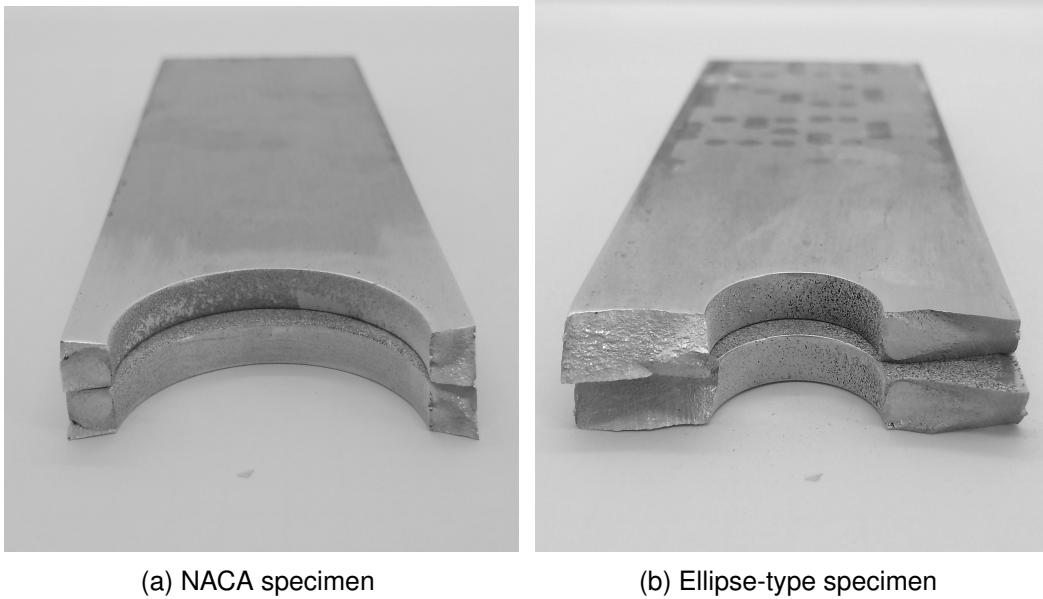


Figure 11 – Examples of failed specimens. There is an area of fatigue crack growth with the crack path perpendicular to the loading direction followed by a residual strength fracture.

notched specimens with lower  $\chi$ , the theory of descending lifetime with reduction in  $\chi$  cannot be verified. The obtained regression shows a slightly larger life expectancy for the elliptical hole specimens compared to the NACA design, despite the higher  $\chi$  of the NACA design, for shorter fatigue lives. However, the difference is small and reverses at higher  $N_f$  because of the slightly different gradients of the regression lines. The difference in the mean between the samples is considered in the next subsection to statistically determine whether the samples can be clearly separated.

Relating back to the existing semi-empirical theories describing the benefit of stress gradients, there seems to be a significant under-estimation of the obtainable increase in fatigue life in specimens. It is conceivable that the early theories erred on the side of conservative estimations to increase safety and account for other effects, e.g. corrosion or manufacturing-induced reduced surface quality at cut-outs. A last possibility is that – without mentioning – a size correction was introduced to account for the larger size of cut-outs in service compared to laboratory specimens. However,  $\chi$  already accounts for size as its unit is 1/mm and larger structures will have smaller  $\chi$  with the same geometry and stress concentration. This gives us reason to believe that there is scope for further investigation into the possibility of enhancing the current  $\chi$  definition and increase the accuracy of fatigue life predictions.

Table 3 gives the Basquin coefficients for the test data. In addition, the normalised load amplitude at  $N_f=1 \times 10^5$  is reported. To compare with the support factor from FKM, the experimental fatigue factor  $n_{exp}$  is introduced. It is defined as the ratio of normalised load amplitude in the notched specimens to the normalised load amplitude of the unnotched specimen at the same  $N_f$  to

$$n_{exp} = \frac{L_{norm,a,notched}(N_f)}{L_{norm,a,K_t=1.0}(N_f)} \quad (6)$$

Because of the slightly different Parameter  $b$ , this factor is not constant over the high cycle fatigue range. It may be questioned, whether there are different gradients in the S-N curve for the same material when considering local stresses. This is not considered in this paper and scope for future work.

For the unnotched specimen, the support and fatigue factors are defined as unity. For the notched specimens, values for  $n_\sigma$  are obtained according to FKM [10], where relative stress gradient and material are considered. It can be seen that when compared to the experimental data, the support factors  $n_\sigma$  are very conservative for the tested material. Obtained values for  $n_{exp}$  are between 9 and 17% higher than the literature data. Similarly conservative are the theories of Peterson and Siebel

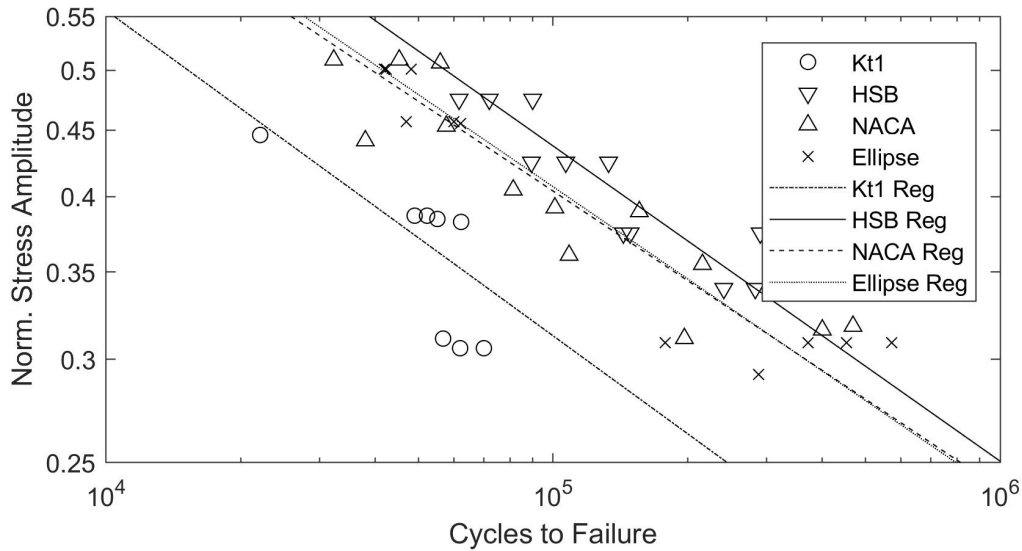


Figure 12 – S-N curves for the tested specimens.

Specimen	Parameter $a$	Parameter $b$	$L_{norm,a}$ at $N_f=1 \times 10^5$	$n_{exp}$ (exp.)	$n_{\sigma}$ (FKM)
$K_t=1.0$	13.401	4.006	0.309	1.000	1.000
HSB	13.029	4.134	0.432	1.400	1.206
NACA	13.254	4.376	0.380	1.231	1.129
Ellipse	13.137	4.259	0.402	1.302	1.110

Table 3 – S-N curve regression parameters and expected cycles to failure for a representative load.

and Stieler. The experimental data thus shows that significant design potential and fatigue life is not utilised in the currently applied theories. Nevertheless, there is still some research required to ensure that the results obtained for the present material is applicable to other aluminium and further engineering materials also.

Comparison of NACA and Ellipse data shows furthermore a reversed trend in fatigue life extension. Whilst theories relying on  $\chi$  alone assign the NACA specimen a longer fatigue life than the elliptical specimen, the experimental data at this  $N_f$  attributes the Ellipse-design a higher fatigue life. The S-N chart shows however a reversing trend in the regression S-N lines between the two specimens, meaning that at a higher  $N_f$ -value the result is different. Generally, there is little difference between these two specimen designs, and the next subsection investigates whether there is statistical significance in the different mean values of their distributions.

### 3.3 Statistical Evaluation

To confirm the statistical significance of the results, a distribution of results is assumed. In accordance with the literature and industrial practice [15, 16], the data is assumed to be log-normal distributed. For the presented fatigue test data, estimated values of the mean,  $\bar{X}$  and standard deviation  $S$  of the distribution are obtained at one fictitious load level, to which all data points are shifted using the Basquin parameters calculated earlier. The resulting values are reported in Table 4 for a load level of  $L_{norm,a}=0.25$ . The index  $i$  can take the values  $K$ ,  $H$ ,  $N$ , and  $E$  for unnotched, HSB design, NACA design, and Ellipse, respectively.

Note that the mean value of the  $K_t=1.0$ -specimen is much lower than for the notched specimens. NACA and Ellipse mean values and standard deviations are similar, whilst the HSB design shows the highest mean life expectancy together with the lowest standard deviation of results. This supports the previous results from the S-N curve and gives additional information on the dispersion of the data, which shows a reducing trend with higher  $\chi$  values.

With the estimates of  $\bar{X}$  and  $S$  for each test, the t-Test for the difference in mean values is calculated

Specimen	$n_i$	$\bar{X}_i$	$S_i$
$K_t=1.0$	12	5.471	0.266
HSB	12	5.997	0.095
NACA	13	5.832	0.155
Ellipse	11	5.891	0.145

Table 4 – Statistical estimates for mean and standard deviations for the samples.  $i$  is the suffix of each specimen design.

Test	Testing for:	$df$	$t_{95}(df)$	t-value	Negated
$t_{KN}$	$\bar{X}_K = \bar{X}_N$	21	1.721	4.109	Yes
$t_{KE}$	$\bar{X}_K = \bar{X}_E$	19	1.729	4.750	Yes
$t_{EN}$	$\bar{X}_E = \bar{X}_N$	20	1.725	0.954	No
$t_{EH}$	$\bar{X}_E = \bar{X}_H$	19	1.729	2.072	Yes
$t_{NH}$	$\bar{X}_N = \bar{X}_H$	21	1.721	3.250	Yes

Table 5 – Results of t-Test for equal means of the tests. Negated tests mean that the means are different at a significance level  $\alpha=0.05$ .

with the formula

$$t_{ij} = \frac{\bar{X}_i - \bar{X}_j}{\sqrt{\frac{S_i^2}{n_i} + \frac{S_j^2}{n_j}}} \quad (7)$$

and compared with tabulated t-values [17] using the degrees of freedom  $df$

$$df = n_i + n_j - 4 \quad (8)$$

for a desired significance level of  $\alpha=0.05$  in a one-sided test. The one-sided test is used as the hypothesis of equal means is tested against the alternative that  $N_f$  reduces with  $\chi$ .

The resulting t-values are given in Table 5. The obtained t-values are much higher than the  $\alpha=0.05$  significance level for the comparisons of elliptical and NACA designs to the  $K_t=1.0$  data,  $t_{KE}$  and  $t_{KN}$ , respectively. Furthermore, the HSB design is shown to have a higher mean than elliptical and NACA designs by the same significance level, see  $t_{EH}$  and  $t_{NH}$ , respectively. Only the test between elliptical and NACA data ( $t_{EN}$ ) is not negated, meaning the hypothesis of equal means can be accepted for the current data. Therefore, statistically, there is no difference between the NACA specimen and elliptical specimen S-N data. More analysis is necessary to evaluate differences at lower  $\chi$  values.

#### 4. Conclusions

In conclusion, in this contribution, the increase in fatigue life at stress concentrations with larger  $\chi$  was experimentally confirmed. The effect of the stress gradient on life increase is however larger than predicted in existing formulas. Furthermore, test series do not consequently follow the trend and it is hypothesised that another mechanism, potentially related to the size of the highly stressed area, should be considered. The data from two designs is not sufficient to establish a general theory, and further experimental testing is envisaged to strengthen the conclusions and establish an enhanced fatigue life correction method at stress concentrations.

#### 5. Contact Author Email Address

mailto: stefan.sieberer@jku.at

#### 6. Copyright Statement

The authors confirm that they, and/or their company or organization, hold copyright on all of the original material included in this paper. The authors also confirm that they have obtained permission, from the copyright holder of any third party material included in this paper, to publish it as part of their paper. The authors confirm that they give permission, or have obtained permission from the copyright holder of this paper, for the publication and distribution of this paper as part of the ICAS proceedings or as individual off-prints from the proceedings.

## References

- [1] Kirsch G. Die Theorie der Elastizität und die Bedürfnisse der Festigkeitslehre. *Zeitschrift des VDI*, Vol. 42, pp 797-807, 1898.
- [2] Howland RCJ. On the Stresses in the Neighbourhood of a Circular Hole in a Strip under Tension. *Phil Trans Royal Soc*, Vol. 229, pp 49-86, 1930.
- [3] Filippini M. Stress gradient calculations at notches. *Int J Fatigue*, Vol. 22 pp 397–409, 2009.
- [4] Koiter WT. An elementary solution of two stress concentration problems in the neighbourhood of a hole, *Quarterly of Appl Math*, Vol. 15, pp 303-308, 1957.
- [5] Neuber H. *Kerbspannungslehre*. 3rd edition, Springer, 2001.
- [6] Siebel E, Stieler M. Ungleichförmige Spannungsverteilung bei schwingender Beanspruchung. *VDI Zeitschrift*, Vol. 97, pp 121-126, 1955.
- [7] Pilkey WD. *Peterson's Stress Concentration Factors*. J Wiley and Sons, 2007.
- [8] Radaj D, Vormwald M. *Ermüdungsfestigkeit*. 3rd edition, Springer, 2007.
- [9] Schijve J. *Fatigue of Structures and Materials*. 2nd edition, Springer, 2009.
- [10] Forschungskuratorium Maschinenbau (FKM) *Rechnerischer Festigkeitsnachweis für Maschinenbauteile*. 5th edition, VDMA Verlag, 2003.
- [11] Industrieausschuss Strukturberechnung (IASB). HSB Sheet 63111-01, 1986.
- [12] National Advisory Committee for Aeronautics (NACA). Technical Note TN2389, 1951.
- [13] Sieberer S, Viehböck E G, Schagerl M. Optical stress concentration and stress gradient monitoring during elasto-plastic fatigue tests with Digital Image Correlation . *Materials Today: Proceedings*, Proceedings of DAS37, 21st-24th Sept 2021, Linz, Austria, pp 1-11, 2022.
- [14] Haibach E. *Betriebsfestigkeit*. Springer-Verlag Berlin Heidelberg New York, 2006.
- [15] Masendorf R, Müller C. Execution and evaluation of cyclic tests at constant load amplitudes - DIN50100:2016. *Materials Testing*, Vol. 60, No. 10, pp 961-968, 2018.
- [16] Müller C, Wächter M, Masendorf R, Esderts A. Distribution functions for the linear region of the S-N curve. *Materials Testing*, Vol. 59, No. 7-8, pp 625-629, 2017.
- [17] Dixon WJ, Massey FJ. *Introduction to Statistical Analysis*. 4th edition, McGraw-Hill, 1983.